The EMBO Journal (2007) 26, 559–566 | © 2007 European Molecular Biology Organization | All Rights Reserved 0261-4189/07
www.embojournal.org

THE
EMBO
JOURNAL

The dynamin middle domain is critical for tetramerization and higher-order self-assembly

Rajesh Ramachandran[1], Mark Surka[1], Joshua S Chappie[1], Douglas M Fowler[2], Ted R Foss[2], Byeong Doo Song[1] and Sandra L Schmid[1,*]

[1]Department of Cell Biology, The Scripps Research Institute, La Jolla, CA, USA and [2]Department of Chemistry and The Skaggs Institute of Chemical Biology, The Scripps Research Institute, La Jolla, CA, USA

The large multidomain GTPase dynamin self-assembles around the necks of deeply invaginated coated pits at the plasma membrane and catalyzes vesicle scission by mechanisms that are not yet completely understood. Although a structural role for the 'middle' domain in dynamin function has been suggested, it has not been experimentally established. Furthermore, it is not clear whether this putative function pertains to dynamin structure in the unassembled state or to its higher-order self-assembly or both. Here, we demonstrate that two mutations in this domain, R361S and R399A, disrupt the tetrameric structure of dynamin in the unassembled state and impair its ability to stably bind to and nucleate higher-order self-assembly on membranes. Consequently, these mutations also impair dynamin's assembly-dependent stimulated GTPase activity.

The EMBO Journal (2007) **26,** 559–566. doi:10.1038/sj.emboj.7601491; Published online 14 December 2006
Subject Categories: structural biology
Keywords: dynamin; endocytosis; GTPase; middle domain; structure

Introduction

The large GTPase dynamin (~100 kDa) plays a critical role in clathrin-mediated endocytosis (Hinshaw, 2000; Conner and Schmid, 2003; Praefcke and McMahon, 2004). Dynamin self-assembles into collar-like structures around the necks of deeply invaginated coated pits at the plasma membrane and by mechanisms not yet clear mediates the pinching-off of coated vesicles into the cytoplasm (Sever *et al*, 2000b; Song and Schmid, 2003). *In vitro*, dynamin forms supramolecular structures consisting of rings and spirals either in low ionic strength buffers (<50 mM salt) (Hinshaw and Schmid, 1995) or at physiological ionic strength (150 mM salt) onto negatively charged lipid templates to generate dynamin-encircled lipid tubules that are reminiscent of the collars observed *in vivo* (Sweitzer and Hinshaw, 1998; Stowell *et al*, 1999).

*Corresponding author. Department of Cell Biology, The Scripps Research Institute, 10550 N Torrey Pines Road, La Jolla, CA 92037, USA. Tel.: +1 858 784 2311; Fax: +1 858 784 9126;
E-mail: slschmid@scripps.edu

Received: 18 July 2006; accepted: 15 November 2006; published online: 14 December 2006

Dynamin exhibits stimulated GTPase activity upon self-assembly and undergoes appreciable conformational changes during its GTP hydrolysis cycle (Sever *et al*, 1999; Stowell *et al*, 1999; Chen *et al*, 2004). Based on these observations, self-assembled dynamin has been proposed to function as a mechanochemical enzyme that employs nucleotide-dependent conformational changes to either constrict, stretch or twist the underlying membrane bilayer in order to sever the coated pit neck at the plasma membrane (Hinshaw and Schmid, 1995; Sweitzer and Hinshaw, 1998; Stowell *et al*, 1999; Chen *et al*, 2004; Roux *et al*, 2006). Other data suggest that unassembled dynamin functions as a regulatory molecule controlling earlier stages of coated vesicle formation (Sever *et al*, 1999, 2000a). These two models for dynamin function are not mutually exclusive, and recent evidence suggests that both assembly-stimulated and assembly-independent GTPase activities of dynamin are critical for clathrin-mediated endocytosis (Song *et al*, 2004a; Narayanan *et al*, 2005).

Dynamin has a modular structure comprised of an N-terminal GTPase domain (residues 1–300), a pleckstrin homology (PH) domain (residues 521–623) responsible for membrane binding, a GTPase effector domain (GED; residues 624–750) involved in self-assembly and that also serves as an internal, assembly-dependent GTPase-activating protein and a C-terminal proline/arginine-rich domain (residues 751–864) that binds to numerous, functionally diverse SH3 domain-containing proteins that participate in endocytosis (Hinshaw, 2000). Apart from these, dynamin also contains a 'middle' domain (residues 301–520) of ill-defined function that lacks sequence homology to any known structural motif. The N-terminal half of this domain, which contains a predicted coiled-coil region (residues 320–350), is significantly more conserved than the C-terminal half between dynamin isoforms (Warnock and Schmid, 1996).

A potential role for the middle domain in dynamin self-assembly has been suggested based on two independent studies conducted on isolated fragments of this segment. Circular dichroism (CD) spectroscopy and sedimentation equilibrium analyses have demonstrated that a synthetic peptide derived from the N-terminal half of the middle domain (residues 323–352) adopts an α-helical coiled-coil structure and forms stable tetramers in solution (Okamoto *et al*, 1999), whereas yeast two-hybrid analyses have revealed that the middle domain makes extensive contacts with the self-assembling GED (Smirnova *et al*, 1999). Recent cryo-EM studies have suggested that a 'stalk' presumably composed of the GED and the middle domain mediates intermolecular interactions in self-assembled dynamin (Zhang and Hinshaw, 2001). Although these studies predict a structural role for the middle domain in dynamin function, it is not known whether these interactions pertain to dynamin's tertiary/quaternary structure in the unassembled state or to its supramolecular assembly or both. Furthermore, the quaternary structure of dynamin in the unassembled state has not

been unambiguously established and remains a matter of debate. In its native state, dynamin has been reported to exist either as monomers (Binns *et al*, 1999), dimers (Tuma and Collins, 1995) or tetramers (Muhlberg *et al*, 1997). Thus, the role of the middle domain within the context of tertiary, quaternary and higher-order structures still remains to be experimentally tested in the context of a full-length dynamin molecule.

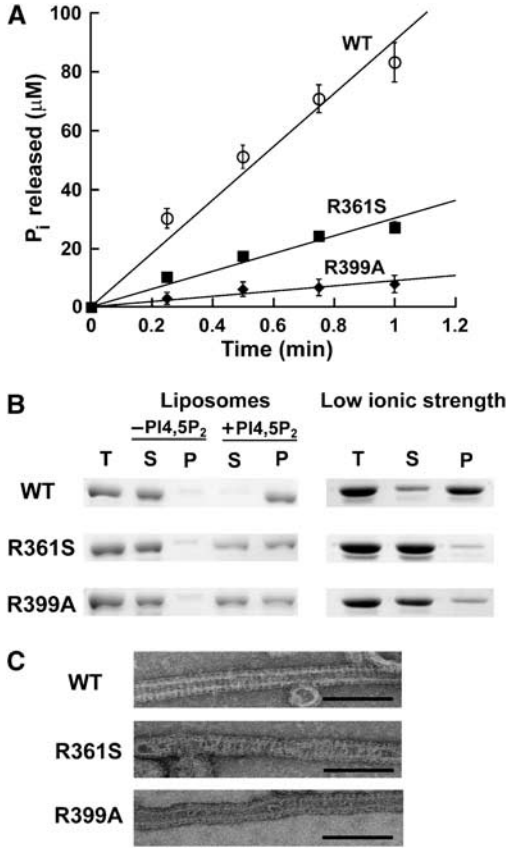

Figure 1 Dyn1-R361S and Dyn1-R399A are defective in self-assembly. (**A**) GTPase activities of 0.5 μM Dyn1-WT (○), Dyn-R361S (■) or Dyn1-R399A (◆) after pre-incubation with $PI4,5P_2$-containing liposomes (150 μM lipid) was measured at 37°C, as described under Materials and methods. The concentration of P_i released is plotted as a function of time. The average values of at least four independent experiments are shown with standard deviations, as indicated. (**B**) Self-assembly of dynamin (1 μM protein) on liposomes (300 μM lipid) with or without $PI4,5P_2$, or at low ionic strength (no salt), was examined by sedimentation followed by SDS–PAGE analysis of the supernatant (S) and pellet (P) fractions as described under Materials and methods; total protein (T). (**C**) Electron micrographs of Dyn1-WT, Dyn1-R361S and Dyn1-R399A (1 mg/ml protein) self-assembled on $PI4,5P_2$-containing liposomes (1 mg/ml lipid) were obtained as described under Materials and methods. Scale bar, 200 nm.

In order to elucidate the role of the middle domain in dynamin structure and function, we have introduced and characterized two mutations, R361S and R399A, in the conserved N-terminal half of this domain. These mutations disrupt dynamin's quaternary structure in the unassembled state and consequently impair its ability to stably bind to, and nucleate self-assembly on, membranes. Thus, we establish that the middle domain is an oligomerization domain required for dynamin's quaternary structure in the unassembled state and also for higher-order self-assembly.

Results

Dyn1-R361S and Dyn1-R399A are defective in self-assembly

Dynamin self-assembles into higher-order structures in low ionic strength buffers (<50 mM salt) even in the absence of a lipid template, pointing to the involvement of charged residues in protein–protein interactions (Hinshaw and Schmid, 1995). Hence, we chose to substitute two conserved arginines at positions 361 and 399 in the N-terminal half of the middle domain with uncharged residues, serine (R361S) and alanine (R399A) respectively, with the expectation that these mutations would adversely affect higher-order self-assembly. The CD and Trp emission spectra of Dyn1-R361S and Dyn1-R399A were identical to those of Dyn1-WT (wild type) suggesting that the tertiary structure of dynamin was not significantly perturbed by these mutations (Supplementary Figure 1).

Formation of higher-order structures consisting of rings and spirals onto negatively charged lipid templates including L-α-phosphatidylinositol-4,5-bisphosphate ($PI4,5P_2$)-containing liposomes enhances dynamin's GTP hydrolysis rate up to 100-fold, a lack of or reduction of which may imply an intrinsic defect in self-assembly (Song *et al*, 2004b). To test whether substitutions R361S and R399A affect dynamin's assembly-dependent GTPase stimulation, we determined the GTPase activities of Dyn1-R361S and Dyn1-R399A upon incubation with 15 mol% $PI4,5P_2$-containing liposomes (Figure 1A). The stimulated GTPase activities of Dyn1-R361S and Dyn1-R399A were reduced 3- and 10-fold, respectively, when compared with Dyn1-WT (Table I), suggesting that these mutants may indeed be impaired in higher-order self-assembly. More drastic reductions in stimulated GTPase activities were observed for Dyn1-R361S and Dyn1-R399A upon incubation with 100 mol% phosphatidylserine (PS) liposomes, another negatively charged lipid template that supports dynamin self-assembly (Supplementary Figure 2).

The apparent reduction in the assembly-stimulated GTPase activities of Dyn1-R361S and Dyn1-R399A can be accounted for either by a loss of catalytic activity but not self-assembly or by impaired self-assembly that ultimately affects GTPase

Table I Properties of Dyn1-WT, Dyn1-R361S and Dyn1-R399A

Parameters	Dyn1-WT	Dyn1-R361S	Dyn1-R399A
Assembly-dependent GTPase activity (μM/min)[a]	90.3±6.9	30.1±1.7	8.9±3.5
Sedimentation coefficient (S or Svedbergs)[b]	~10–12	~6	~6
Molecular mass by MALLS (kDa)	~350	~170	~180
Estimated number of subunits[c]	4	2	2

[a]Obtained by linear least-square analysis of data from at least four independent experiments.
[b]Predominant species.
[c]Rounded to the nearest subunit composition.

activity. To directly test these possibilities, we next determined the ability of these mutants to bind to, and form higher-order structures on, PI4,5P_2-containing liposomes that are readily sedimentable by centrifugation. Although nearly all of Dyn1-WT was recovered by sedimentation in the presence of these liposomes, only ~50% of each of the mutants was sedimentable (Figure 1B), confirming that Dyn1-R361S and Dyn1-R399A are impaired in membrane binding. In control experiments with liposomes lacking PI4,5P_2 or PS, neither Dyn1-WT nor the mutants were sedimentable, reflecting dynamin's specificity towards negatively charged membranes. Consistent with a defect also in self-assembly, both Dyn1-R361S and Dyn1-R399A were impaired in assembling into sedimentable, higher-order structures under low ionic strength conditions that otherwise promote Dyn1-WT assembly even in the absence of a lipid template (Figure 1B).

The nearly 50% reduction in Dyn1-R361S and Dyn1-R399A binding to PI4,5P_2-containing liposomes is less severe than the ~70 and 90% reductions in their assembly-stimulated GTPase activities, respectively (Figure 1A and B). One possible explanation for this apparent inconsistency is a defect in the higher-order structures formed by membrane-bound Dyn1-R361S and Dyn1-R399A that results in a less effective stimulation of GTP hydrolysis. To determine whether the higher-order structures formed by Dyn1-R361S and Dyn1-R399A on PI4,5P_2-containing liposomes are similar to those formed by Dyn1-WT, we visualized them by negative-stain electron microscopy. In contrast to Dyn1-WT, which deformed spherical liposomes into lipid tubules of nearly uniform diameter encircled by well-organized stacks of a polymeric dynamin spiral, both Dyn1-R361S and Dyn1-R399A formed lipid tubules of variable diameter along the tubule length encircled by disordered rungs of a dynamin spiral (Figure 1C). Taken together, these data suggest that Dyn1-R361S and Dyn1-R399A are not only impaired in membrane binding, but also form defective higher-order structures when self-assembled on membranes.

Dyn1-R361S and Dyn1-R399A are assembly-defective dimers

Dynamin binds to PI4,5P_2-containing membranes via its PH domain. Previous studies have shown that the affinity of an isolated dynamin PH domain for the phosphoinositide headgroup is low, and therefore, stable binding of dynamin to a PI4,5P_2-containing membrane surface requires the high avidity interactions provided by its oligomerization (Klein *et al*, 1998; Lemmon and Ferguson, 2000). Sedimentation equilibrium experiments have shown that dynamin in the unassembled state exists in dynamic equilibrium between monomeric and tetrameric states, with the tetramer thermodynamically favored over the monomer (Binns *et al*, 1999). As dynamin in the tetrameric state is expected to exhibit a higher avidity for the target membrane than a monomer or a dimer, we reasoned that impaired membrane binding in Dyn1-R361S and Dyn1-R399A could be due to a perturbation in dynamin quaternary structure that significantly reduces its avidity for the target membrane.

To test whether Dyn1-R361S and Dyn1-R399A have disrupted quaternary structures in their unassembled state, we initially determined their sedimentation coefficients (S) by sedimentation velocity analytical ultracentrifugation. In contrast to Dyn1-WT, which sedimented at ~10–12 S, both Dyn1-R361S and Dyn1-R399A sedimented predominantly at ~6 S with only minor fractions at 10–12 S corresponding to that of the WT (Figure 2A). These data indicated that Dyn1-R361S and Dyn1-R399A are indeed disrupted in quaternary structure with the equilibrium shifted in favor of smaller species, presumably monomers or dimers.

Accurate determination of the quaternary structure of Dyn1-R361S and Dyn1-R399A by sedimentation equilibrium analytical ultracentrifugation, as determined previously for Dyn1-WT (Muhlberg *et al*, 1997), was precluded owing to a slow rate of dynamin microaggregation in our samples (see void volume in Figure 2B). To overcome this limitation, both WT and mutant dynamin samples were resolved by size-exclusion chromatography (SEC; Figure 2B) and the major species in the included volume were analyzed by on-line multiangle laser light scattering (MALLS), a technique now widely used for unambiguous molecular mass determinations (Wen *et al*, 1996; Andersson *et al*, 2003; Ye, 2006). Unlike SEC, which relies on data based on relative standards and is influenced by molecular shape or sedimentation equilibrium analytical ultracentrifugation, which is time consuming resulting in protein aggregation during the course of the experiment, this combination of SEC and MALLS (SEC-MALLS) is relatively quick and determines the average molecular mass of each eluted fraction directly without calibration against standards or assumptions of molecular

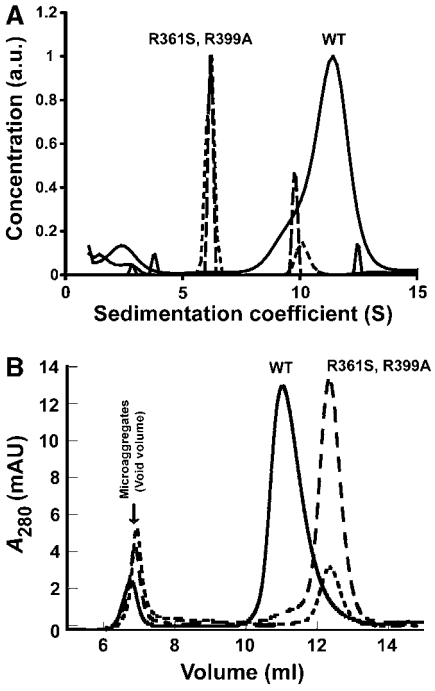

Figure 2 Dyn1-R361S and Dyn1-R399A are assembly-defective dimers. (**A**) Sedimentation coefficients (*S*) of Dyn1-WT (solid line), Dyn1-R361S (short dashes) and Dyn1-R399A (long dashes) at 5 μM each were obtained as described under Materials and methods and are plotted here as a function of the relative concentration of each species. (**B**) SEC elution profiles for Dyn1-WT (solid line), Dyn1-R361S (short dashes) and Dyn1-R399A (long dashes) run through a Superose 6 10/30 HR (Amersham Biosciences) column were obtained as described under Materials and methods. Protein absorbance at 280 nm (A_{280}) in milli-absorbance units (mAU) is plotted here as a function of elution volume (ml). Arrowhead points to the elution of dynamin microaggregates in the void volume.

shape and size. SEC-MALLS data analyses unambiguously showed that Dyn1-R361S and Dyn1-R399A are predominantly dimers in contrast to Dyn1-WT tetramers (Table I). Thus, these data reveal that R361 and R399 in the middle domain are critical for establishing dynamin tetrameric structure in the unassembled state.

Dyn1-R361S and Dyn1-R399A exhibit impaired cooperativity in self-assembly

Previous studies have shown that dynamin's GTPase activity increases nonlinearly or sigmoidally with increasing protein concentration, reflecting positive cooperativity in higher-order dynamin–dynamin interactions that disproportionately enhances GTPase activity (Warnock *et al*, 1996; Song *et al*, 2004b). To determine whether the assembly defect in Dyn1-R361S and Dyn1-R399A is due to impaired positive cooperativity, we determined their GTP hydrolysis rates with increasing protein concentration and at low ionic strength (no salt) that favors higher-order self-assembly. Whereas the GTP hydrolysis rates of Dyn1-WT increased sigmoidally with increasing protein concentration, as expected, only a linear response was elicited from Dyn1-R361S and Dyn1-R399A, indicating impaired positive cooperativity in dynamin–dynamin interactions that promote higher-order self-assembly (Figure 3).

Dynamin's basal GTPase activation is not rate-limited by nucleation

In recent studies using a coupled assay to measure the kinetics of GTP hydrolysis of either the yeast mitochondrial dynamin-related protein, Dnm1, or Dyn1-WT, a kinetic 'lag' was observed upon dilution of these proteins into low ionic strength buffer to trigger self-assembly before steady-state GTP hydrolysis rates were achieved (Ingerman *et al*, 2005; Sever *et al*, 2006). The duration of the lag decreased with increasing protein concentration, suggesting that it represented a rate-limiting nucleation event also cooperative with respect to GTP concentration. Consistent with this interpretation, no lag was detected when assaying middle domain mutants, Dnm1G385D or Dyn1-I690K, which coincidentally also exist as assembly-defective dimers in solution (Ingerman *et al*, 2005; Sever *et al*, 2006).

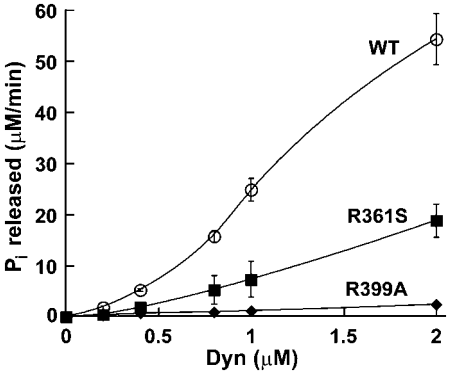

Figure 3 Dyn1-R361S and Dyn1-R399A dimers exhibit impaired cooperativity in self-assembly. GTP hydrolysis rates of Dyn1-WT (○), Dyn-R361S (■) or Dyn1-R399A (◆) at low ionic strength (no salt) were determined at 37°C as described under Materials and methods, and are plotted as a function of dynamin concentration. The GTPase activities of Dyn1-R361S and Dyn1-R399A are linearly proportional to their concentration in contrast to Dyn1-WT, which exhibits sigmoidal behavior. The average values of at least three independent experiments are shown along with standard deviations.

We have used this coupled assay to examine the kinetics of basal GTP hydrolysis by Dyn1-WT in comparison to Dyn1-R399A, which exhibited the greatest defect in self-assembly (Figures 1A, B and 3). Interestingly, we also detected a pronounced kinetic lag for Dyn1-WT even when assayed at physiological ionic strength (150 mM KCl), a condition that does not favor dynamin self-assembly in the absence of an appropriate lipid template (Figure 4A and Table II). In contrast to previous studies conducted at low ionic strength, we also detected a lag with the assembly-defective Dyn1-R399A mutant (Figure 4B and Table II). No lag was detected when the dynamin GTPase domain alone (residues 1–307) was subjected to this assay, indicating that it is not an artifact of assay conditions and also suggesting that the molecular events occurring during the lag phase involve domains other than or in addition to the GTPase (Supplementary Figure 3).

If this lag represents a rate-limiting nucleation event as suggested for dynamin at low ionic strength (Ingerman *et al*, 2005; Sever *et al*, 2006), and if the steady-state basal rate of GTP hydrolysis at physiological ionic strength is also limited by dynamin–dynamin higher-order interactions, then one would expect a substantial reduction in the lag period and an exponential increase in the rate of basal GTP hydrolysis with increasing protein concentration. Contrary to this scenario, there was no significant decrease in the lag period for either Dyn1-WT or Dyn1-R399A with increasing protein concentration (Table II). In addition, the specific activity of Dyn1-WT merely doubled with a three-fold increase in protein concentration (from 2 to 6 μM) showing a less than linear dependence on it (Table II). Similarly, Dyn1-R399A, which had slightly higher rates of basal GTP hydrolysis than Dyn1-WT, exhibited only a modest concentration-dependent increase in its specific activity (Table II). These data suggest that the basal GTPase activity of dynamin at physiological ionic strength is independent of higher-order protein–protein interactions.

To directly probe for evidence of higher-order dynamin–dynamin interactions under these conditions, we developed and employed a fluorescence-based assay that monitors dynamin self-assembly in real time. Here, Dyn1-WT and Dyn1-R399A were both labeled with the thiol-reactive BODIPY dye (BODIPY-FL C_1-IA, hereafter shortened to BODIPY) that selectively and covalently modifies reactive Cys residues on the protein surface (out of a total of seven). As statistical proximity of two excited-state BODIPY fluorophores within a critical radius of ~25 Å leads to self-quenching (Dahim *et al*, 2002; Fernandes *et al*, 2003), the potential decrease in BODIPY fluorescence intensity upon Dyn^{BODIPY}–Dyn^{BODIPY} interactions was used as an index of dynamin self-assembly. Control experiments established that BODIPY labeling did not alter the GTPase activity or self-assembly properties of the respective proteins (data not shown). As expected, self-assembly of Dyn1-WT^{BODIPY} on PI4,5P_2-containing membranes resulted in nearly 15% quenching of BODIPY emission intensity, whereas, on the other hand, incubation of Dyn1-$R399A^{BODIPY}$ with these membranes did not show any significant quenching, also

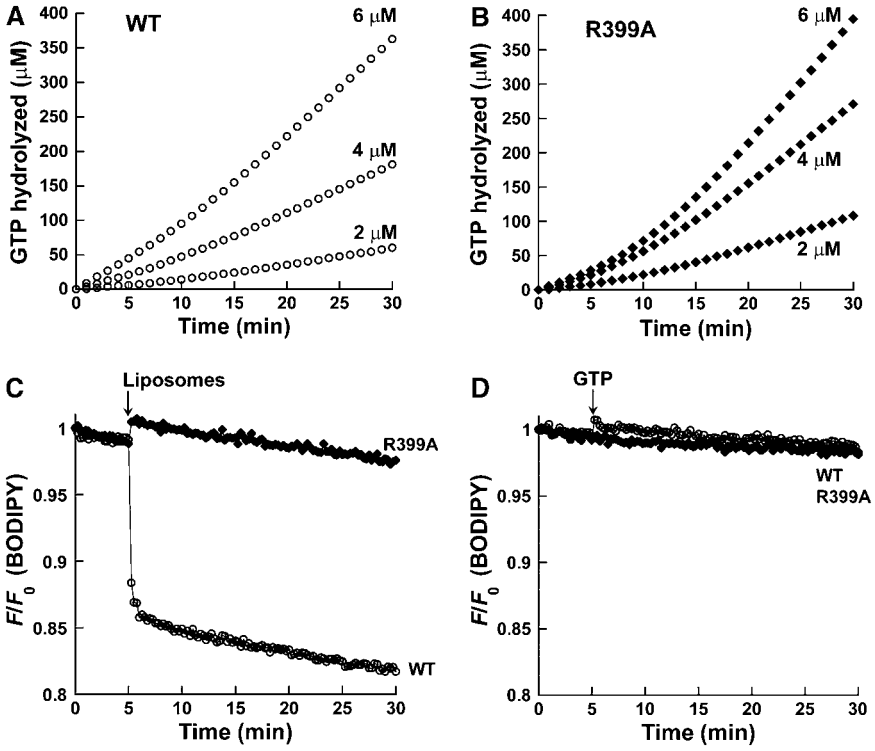

Figure 4 Activation of dynamin basal GTPase is not due to nucleation. (**A, B**) The kinetics of basal GTP hydrolysis in Dyn1-WT (○) or Dyn1-R399A (◆) at 2, 4 and 6 μM protein concentration was measured at 37°C using the GTP regenerating system as described under Materials and methods. The concentration of GTP hydrolyzed and released is plotted as a function of time. The average values of at least three independent experiments are shown. (**C, D**) Time-dependent emission intensity profiles for 0.1 μM Dyn1-WT^{BODIPY} (○) and Dyn1-R399A^{BODIPY} (◆) before and upon addition (arrowhead) of either GTP (1 mM final) or liposomes (30 μM final) were obtained as described under Materials and methods. BODIPY was excited at 490 nm and emission was monitored at 510 nm. F_0 is the initial intensity of BODIPY at time '0' and F is its intensity at time '*t*'.

Table II Kinetic characterization of Dyn1-WT and Dyn1-R399A

[Dyn] (μM)	Dyn1-WT	Dyn1-R399A
	Kinetic lag (min)[a]	
2	5.8±1.4	6.9±0.1
4	4.4±1.3	6.8±0.1
6	4.4±0.1	7.8±0.9
	Steady-state basal specific activity (min^{-1})[b]	
2	1.2±0.1	2.3±0.1
4	1.8±0.1	2.9±0.2
6	2.4±0.1	2.9±0.1

[a]Obtained from at least three independent experiments by linear extrapolation of the slope of steady-state basal GTP hydrolysis to the *x*-axis. Differences in lag for Dyn-WT and Dyn1-R399A at different concentrations were within experimental error and are not significant.
[b]Obtained by linear least-square analysis of data from at least three independent experiments.

consistent with the defect in its higher-order self-assembly (Figure 4C). The apparent lack of ordered Dyn1-R399A self-assembly upon incubation with PI4,5P_2-containing membranes (Figures 1C and 4C) also correlated well with the nearly 90% reduction in its stimulated GTPase activity despite 50% binding to these membranes (Figure 1B).

Using this assay, we then determined whether dynamin self-assembly or nucleation ensued upon GTP addition. Upon GTP addition, neither Dyn1-WT^{BODIPY} nor Dyn1-R399A^{BODIPY} showed any significant quenching of BODIPY emission intensity, clearly indicating lack of GTP-dependent nucleation or higher-order self-assembly under these conditions (Figure 4D). From these data, we conclude that the activation of the dynamin GTPase observed before steady-state basal GTP hydrolysis is not due to dynamin–dynamin higher-order interactions or nucleation, but perhaps to a slow, allosteric conformational transition in unassembled dynamin relayed between subunits of a tetramer, or a dimer in the case of Dyn1-R399A, presumably by the middle domain and/or the GED that participate in subunit–subunit interactions.

Discussion

The role of the middle domain in dynamin structure and function has remained ill-defined until now. Here, we show that substitution of conserved arginines at positions 361 and 399 in the middle domain disrupts dynamin's tetrameric structure in the unassembled state and consequently impairs its ability to stably bind to and nucleate self-assembly on membranes. Thus, the middle domain functions as an essential oligomerization domain in dynamin self-assembly.

Our results provide four new insights into the mechanism of dynamin self-assembly. First, stable binding of dynamin to target membranes requires the high avidity interactions provided by dynamin tetramerization, evident by impaired membrane binding in Dyn1-R361S and Dyn1-R399A dimers (Figure 1B). Second, the tetramer constitutes the smallest, stable dynamin assembly intermediate that can effectively nucleate further self-assembly, as judged by the impairment of self-assembly in Dyn1-R361S and Dyn1-R399A dimers

(Figures 1B, 3 and 4C). Third, intermolecular interactions involved in dynamin self-assembly are mediated by the middle domain that constitutes at least one of the assembly interfaces in dynamin polymerization. And fourth, GTPase stimulation requires proper register of this assembly interface, as its perturbation in Dyn1-R361S and Dyn1-R399A results in defective higher-order structures and poor stimulation of GTPase activity (Figure 1A and C).

In addition, our findings also resolve two contentious issues regarding the oligomeric state and GTPase activity of unassembled dynamin. Although hydrodynamic analyses have demonstrated that unassembled dynamin remains in dynamic equilibrium between monomeric and tetrameric states, recent low-resolution cryo-EM data suggest that the building block of self-assembled dynamin is instead a dimer (Zhang and Hinshaw, 2001). Based on these observations, it has been suggested that under conditions that favor self-assembly, dynamin shifts from a 'closed' tetramer to an assembly-competent 'open' dimer (Zhang and Hinshaw, 2001). In light of our data that dimers of Dyn1-R361S and Dyn1-R399A are in fact impaired in membrane binding, we propose that the dynamin tetramer is instead a 'dimer of dimers' that can stably bind and nucleate further self-assembly on membranes. Secondly, our finding that Dyn1-WT tetramers and Dyn1-R399A dimers both exhibit robust rates of steady-state GTP hydrolysis that do not correlate with their quaternary structures (Table II) indicates that the basal GTPase activity of dynamin is independent of its higher-order protein–protein interactions (Figure 4A and B and Table II). This basal GTPase activity assumes greater significance in light of the putative role of unassembled dynamin in the early, rate-limiting steps of endocytosis before self-assembly, where dynamin either in the GTP-bound state or in the course of steady-state GTP turnover has been suggested to serve as a kinetic timer that regulates and controls coated pit assembly and maturation (Narayanan *et al*, 2005).

Upon dilution into low ionic strength buffer, both yeast Dnm1 and Dyn1-WT exhibit pronounced kinetic lags preceding steady-state GTP hydrolysis, which has been strictly interpreted to mark a GTP-dependent, rate-limiting nucleation event (Ingerman *et al*, 2005; Sever *et al*, 2006). We interpret these concentration-dependent events to reflect dynamin higher-order assembly and assembly-stimulated GTPase activities. We however also observe similar, but concentration-independent lags for both Dyn1-WT and Dyn1-R399A even at high ionic strength conditions (150 mM KCl) that do not favor dynamin self-assembly in the absence of an appropriate lipid template (Figure 4A and B and Table II), suggesting that this lag observed for basal GTPase activity does not correspond to a GTP-dependent nucleation event. The lack of GTP-dependent nucleation under these conditions was further confirmed by our fluorescence-based measurement of dynamin self-assembly in real time (Figure 4C and D). We therefore suggest that this lag instead reflects an allosteric conformational change in dynamin tetramers, or dimers in the case of Dyn1-R399A, that precedes and activates steady-state basal GTP hydrolysis.

From a structural perspective, our findings establish that the middle domain, in addition to the GED, serves as an assembly interface in dynamin polymerization. Previous studies have shown that GED interacts with the GTPase and the middle domains and also with itself (Sever *et al*, 1999; Smirnova *et al*, 1999). Recent cryo-EM data have suggested that the 'stalk' region in the T-shaped dynamin dimer composed of the GED and the middle domain mediate intermolecular interactions in self-assembled dynamin (Zhang and Hinshaw, 2001). It was recently shown that a self-assembly-defective GED mutant (Dyn1-I690K) that was previously reported to form WT-like tetramers in equilibrium-disrupting crosslinking experiments (Song *et al*, 2004b) exists as a dimer, by analytical ultracentrifugation (Sever *et al*, 2006). Using SEC-MALLS, we have independently verified this finding (our unpublished results). This GED mutant exhibits assembly defects very similar to those of Dyn1-R361S and Dyn1-R399A (Song *et al*, 2004b). In light of these observations, we predict that the middle domain and the GED each present an assembly interface on opposite faces of the dimer stalk that participate in intermolecular interactions along the radial axis of the dynamin spiral.

Materials and methods

Mutagenesis and generation of recombinant baculoviruses

cDNA encoding human dynamin 1 subcloned in pBS II (KS+) (Stratagene) was used as the template for Quikchange mutagenesis (Stratagene). Mutations were confirmed by automated DNA sequencing. The *Bam*HI–*Kpn*I fragment carrying each mutation was then used to replace the corresponding fragment of WT dynamin 1 cDNA subcloned in pVL1393 (AB vector). Recombinant baculoviruses harboring these cDNA constructs were generated by cotransfection of Sf9 insect cells together with BaculoGold linearized baculovirus DNA according to the manufacturer's instructions (Pharmingen).

Dynamin expression and purification

Dynamin was expressed in Tn5 insect cells infected with recombinant baculovirus and purified by affinity chromatography using the amphiphysin II SH3 domain conjugated to glutathione-*S*-transferase (Marks *et al*, 2001). Purified dynamin was dialyzed against storage buffer (20 mM HEPES (pH 7.5), 150 mM KCl, 1 mM EDTA, 1 mM EGTA, 1 mM DTT, 50% v/v glycerol) and stored at −80°C. Addition of glycerol stabilized our dynamin preparations and considerably reduced protein aggregation (Quan and Robinson, 2005). Protein concentration was determined by absorbance at 280 nm using a molar absorptivity coefficient of $58\,790\ M^{-1}\,cm^{-1}$.

The GTPase domain of dynamin (residues 1–307) subcloned in pMAL c2X (NEB) was overexpressed in *Escherichia coli* BL21 (DE3) (Invitrogen) as an N-terminal fusion to the maltose-binding protein (MBP-GTPase) and purified according to NEB's protocol. Purified protein was aliquoted, flash frozen in liquid nitrogen and stored as above. Protein concentration was determined by absorbance at 280 nm using a molar absorptivity coefficient of $73\,800\ M^{-1}\,cm^{-1}$.

Liposome preparation

Liposomes containing either 100 mol% 1,2-dioleoyl-*sn*-glycero-3-phosphocholine (DOPC; Avanti polar lipids) or 100 mol% 1,2-dioleoyl-*sn*-glycero-3-phosphoserine (Avanti polar lipids) or a mixture containing 80 mol% DOPC, 15 mol% porcine brain $PI4,5P_2$ (Avanti polar lipids) and 5 mol% cholesterol (Calbiochem) were prepared by extrusion through 400-nm-pore polycarbonate membranes (Whatman) using an Avanti Mini-extruder, as described earlier (Leonard *et al*, 2005). For sucrose-loaded liposomes, the dried lipid mixture was rehydrated instead in buffer containing 0.3 M sucrose and processed as above.

GTPase assay

Dynamin GTP hydrolysis either at low ionic strength (no KCl) or in the presence of $PI4,5P_2$-containing liposomes at physiological ionic strength (150 mM KCl) was monitored as a function of time using a malachite green-based colorimetric assay that detects released P_i as described earlier (Leonard *et al*, 2005).

The kinetics of basal GTP hydrolysis was measured at physiological ionic strength (150 mM) at 37°C using a coupled assay in which GTP was continuously regenerated, as previously

described (Ingerman *et al*, 2005). Briefly, GTPase assays were performed in 20 mM HEPES (pH 7.5), 150 mM KCl, 5 mM $MgCl_2$, 1 mM phosphoenolpyruvate (PEP), 20 U/ml pyruvate kinase/lactate dehydrogenase, 600 μM NADH and 500 mM GTP in a final volume of 200 μl. Reactions were initiated by the addition of dynamin to a final concentration of 2, 4 or 6 μM to the above mixture and thorough mixing of the contents. Depletion of NADH was measured by monitoring the decrease in absorbance at 340 nm over 90 min using a 96-well plate reader (Synergy HT multidetection microplate reader, BIO-TEK Instruments Inc., Winooski, WT). The change in absorbance over time was used to generate GTP hydrolysis rates under constant GTP concentration.

Sedimentation assay

Dynamin self-assembly on liposomes or under low ionic strength (no KCl) was tested by sedimentation after high-speed centrifugation. For assembly on liposomes, dynamin (1 μM) was incubated with sucrose-loaded liposomes (300 μM lipid with or without $PI4,5P_2$) in 20 mM HEPES, pH 7.5, and 150 mM KCl in a final volume of 50 μl at 37°C for 15 min. Mixtures were then spun at 14 000 r.p.m. (20 800 *g*) for 20 min in a microfuge refrigerated at 4°C to obtain supernatant (S) and pellet (P) fractions. The pellet fraction containing liposomes was resuspended in 50 μl of the same buffer to obtain equal volumes of S and P fractions. For assembly in low ionic strength buffer, dynamin (1 μM), initially in 20 mM HEPES, pH 7.5, and 150 mM KCl, was dialyzed overnight against 20 mM HEPES, pH 7.5, and then fractionated into S and P, as above. Samples were heated at 95°C for 5 min after addition of 10 μl of 6× SDS–PAGE buffer, resolved on an 8% polyacrylamide gel and visualized by Coomassie staining.

Negative staining and electron microscopy

Dynamin (1 mg/ml) was mixed 1:1 (v:v) with $PI4,5P_2$-containing liposomes (1 mg/ml lipid) and incubated at room temperature for 2 h. The mixture was then adsorbed onto carbon-coated grids, washed thoroughly with low-salt buffer (20 mM HEPES, pH 7.5) and stained with 1% uranyl acetate. Images were collected on a film using a Phillips CM200 FEG microscope at 120 kV and a nominal magnification of ×38 000. Representative micrographs were digitized using a Perkin-Elmer Micro-10 1010GM microdensitometer.

Analytical ultracentrifugation

Sedimentation velocity analytical ultracentrifugation was performed on a Beckman XL-I analytical ultracentrifuge using both interference and absorbance optics. AUC cells were constructed with sapphire windows, 1.2-mm charcoal-filled Epon centerpieces, and used with either an An60 Ti four-hole or an An50 Ti eight-hole rotor. Samples (5 μM dynamin in 20 mM HEPES (pH 7.5), 150 mM KCl, 1 mM EDTA, 1 mM EGTA and 1 mM DTT) were equilibrated to 20°C before being spun at 50 000 r.p.m. for 4 h, recording absorbance and interference spectra as quickly as instrumentation allowed (approximately every 2–10 min). Scans were analyzed using the c(s) method in SedFit (Schuck, 2000).

Size-exclusion chromatography and multiangle laser light scattering

Samples (100 μl) of 10 μM dynamin in 20 mM HEPES (pH 7.5), 150 mM KCl, 1 mM EDTA, 1 mM EGTA and 1 mM DTT were fractionated on a Superose 6 10/30 HR (Amersham Biosciences) column equilibrated with 20 mM HEPES, pH 7.5, and 150 mM KCl and analyzed using a DAWN-EOS multiangle light scattering spectrophotometer (Wyatt Technologies, Santa Barbara, CA). Data analysis was accomplished using the ASTRA software package (Wyatt Technologies, Santa Barbara, CA).

BODIPY labeling of dynamin and fluorescence spectroscopy

Dyn1-WT and Dyn1-R399A were labeled with BODIPY using the thiol-reactive reagent, *n*-(4,4-difluoro-5,7-dimethyl-4-bora-3a, 4a-diaza-s-indacene-3-yl)methyl iodoacetamide (BODIPY-FL C1-IA; Invitrogen). BODIPY-FL C1-IA in DMSO was added in a 10-fold molar excess to Dyn1-WT or Dyn1-R399A in buffer containing 20 mM HEPES, pH 7.5, 150 mM KCl and 1 mM EDTA. After 2 h at room temperature, DTT was added to a final concentration of 5 mM to stop the reaction. The reaction mixture was then dialyzed overnight against 20 mM HEPES, pH 7.5, and 150 mM KCl, with several changes of buffer, to separate BODIPY-labeled Dyn from the dye-DTT adduct. The stoichiometry of labeling, determined using a molar absorptivity coefficient of 58 790 M^{-1} cm^{-1} at 280 nm for Dyn and 76 000 M^{-1} cm^{-1} at 502 nm for BODIPY, was 3:1 :: protein:dye. $Dyn1\text{-}WT^{BODIPY}$ and $Dyn1\text{-}R399A^{BODIPY}$ samples were stored on ice and used within a week of preparation.

All intensity measurements were carried out at 25°C using a Fluorolog-3 photon-counting steady-state spectrofluorometer (Jobin Yvon Horiba) with double excitation and double emission monochromators, a cooled PMT housing and a 450 W Xenon lamp. For the acquisition of time-dependent emission intensity profiles for BODIPY, a 0.1 μM sample of either $Dyn1\text{-}WT^{BODIPY}$ or $Dyn1\text{-}R399A^{BODIPY}$ in buffer containing 20 mM HEPES, pH 7.5, 150 mM KCl (for liposome additions) or 20 mM HEPES, pH 7.5, 150 mM KCl, 5 mM $MgCl_2$, 1 mM PEP and 20 U/ml pyruvate kinase/lactate dehydrogenase (for GTP additions) in a final volume of 2.4 ml was continuously stirred and temperature-equilibrated in a 1 cm × 1 cm quartz cuvette. BODIPY was excited at 490 nm (2-nm band pass) and its emission was monitored at 510 nm (2-nm band pass). Data collection was started and recorded at 15 s intervals (5 s signal integration time) until a stable signal was obtained. $PI4,5P_2$-containing liposomes to a final concentration of 30 μM total lipid or GTP to a concentration of 1 mM final was added after 300 s (5 min) and emission intensity monitored for a duration of another 25 min. F_0 is the initial intensity of BODIPY at time '0' and F is its intensity at time 't'. Scatter or signal owing to the addition to liposomes or GTP was <1% of the total emission intensity. The emission intensity of BODIPY upon these additions was corrected for dilution. Before use, cuvette walls were coated overnight with a solution of pure phosphatidylcholine vesicles, prepared by sonication, to minimize protein adsorption to the cuvette wall that can cause artifactual loss of fluorescence intensity (Ye *et al*, 1991).

Supplementary data

Supplementary data are available at *The EMBO Journal* Online (http://www.embojournal.org).

Acknowledgements

We thank Jeffery Kelly for use of his laboratory's instrumentation and Ron Milligan for guidance with electron microscopy. This work was supported by NIH grants R01.GM42455 and R21.CA104046 to SLS and an American Heart Association predoctoral fellowship (AHA-0515009Y) to JSC. This is TSRI manuscript no. 18368.

References

Andersson M, Wittgren B, Wahlund KG (2003) Accuracy in multiangle light scattering measurements for molar mass and radius estimations. Model calculations and experiments. *Anal Chem* **75:** 4279–4291

Binns DD, Barylko B, Grichine N, Atkinson MA, Helms MK, Jameson DM, Eccleston JF, Albanesi JP (1999) Correlation between self-association modes and GTPase activation of dynamin. *J Protein Chem* **18:** 277–290

Chen YJ, Zhang P, Egelman EH, Hinshaw JE (2004) The stalk region of dynamin drives the constriction of dynamin tubes. *Nat Struct Mol Biol* **11:** 574–575

Conner SD, Schmid SL (2003) Regulated portals of entry into the cell. *Nature* **422:** 37–44

Dahim M, Mizuno NK, Li XM, Momsen WE, Momsen MM, Brockman HL (2002) Physical and photophysical characterization of a BODIPY phosphatidylcholine as a membrane probe. *Biophys J* **83:** 1511–1524

Fernandes F, Loura LM, Prieto M, Koehorst R, Spruijt RB, Hemminga MA (2003) Dependence of M13 major coat protein oligomerization and lateral segregation on bilayer composition. *Biophys J* **85:** 2430–2441

Hinshaw JE (2000) Dynamin and its role in membrane fission. *Annu Rev Cell Dev Biol* **16:** 483–519

Hinshaw JE, Schmid SL (1995) Dynamin self-assembles into rings suggesting a mechanism for coated vesicle budding. *Nature* **374:** 190–192

Ingerman E, Perkins EM, Marino M, Mears JA, McCaffery JM, Hinshaw JE, Nunnari J (2005) Dnm1 forms spirals that are structurally tailored to fit mitochondria. *J Cell Biol* **170:** 1021–1027

Klein DE, Lee A, Frank DW, Marks MS, Lemmon MA (1998) The pleckstrin homology domains of dynamin isoforms require oligomerization for high affinity phosphoinositide binding. *J Biol Chem* **273:** 27725–27733

Lemmon MA, Ferguson KM (2000) Signal-dependent membrane targeting by pleckstrin homology (PH) domains. *Biochem J* **350** (Part 1)**:** 1–18

Leonard M, Song BD, Ramachandran R, Schmid SL (2005) Robust colorimetric assays for dynamin's basal and stimulated GTPase activities. *Methods Enzymol* **404:** 490–503

Marks B, Stowell MH, Vallis Y, Mills IG, Gibson A, Hopkins CR, McMahon HT (2001) GTPase activity of dynamin and resulting conformation change are essential for endocytosis. *Nature* **410:** 231–235

Muhlberg AB, Warnock DE, Schmid SL (1997) Domain structure and intramolecular regulation of dynamin GTPase. *EMBO J* **16:** 6676–6683

Narayanan R, Leonard M, Song BD, Schmid SL, Ramaswami M (2005) An internal GAP domain negatively regulates presynaptic dynamin *in vivo*: a two-step model for dynamin function. *J Cell Biol* **169:** 117–126

Okamoto PM, Tripet B, Litowski J, Hodges RS, Vallee RB (1999) Multiple distinct coiled-coils are involved in dynamin self-assembly. *J Biol Chem* **274:** 10277–10286

Praefcke GJ, McMahon HT (2004) The dynamin superfamily: universal membrane tubulation and fission molecules? *Nat Rev Mol Cell Biol* **5:** 133–147

Quan A, Robinson PJ (2005) Rapid purification of native dynamin I and colorimetric GTPase assay. *Methods Enzymol* **404:** 556–569

Roux A, Uyhazi K, Frost A, De Camilli P (2006) GTP-dependent twisting of dynamin implicates constriction and tension in membrane fission. *Nature* **441:** 528–531

Schuck P (2000) Size-distribution analysis of macromolecules by sedimentation velocity ultracentrifugation and lamm equation modeling. *Biophys J* **78:** 1606–1619

Sever S, Damke H, Schmid SL (2000a) Dynamin:GTP controls the formation of constricted coated pits, the rate limiting step in clathrin-mediated endocytosis. *J Cell Biol* **150:** 1137–1148

Sever S, Damke H, Schmid SL (2000b) Garrotes, springs, ratchets, and whips: putting dynamin models to the test. *Traffic* **1:** 385–392

Sever S, Muhlberg AB, Schmid SL (1999) Impairment of dynamin's GAP domain stimulates receptor-mediated endocytosis. *Nature* **398:** 481–486

Sever S, Skoch J, Newmyer S, Ramachandran R, Ko D, McKee M, Bouley R, Ausiello D, Hyman BT, Bacskai BJ (2006) Physical and functional connection between auxilin and dynamin during endocytosis. *EMBO J* **25:** 4163–4174

Smirnova E, Shurland DL, Newman-Smith ED, Pishvaee B, van der Bliek AM (1999) A model for dynamin self-assembly based on binding between three different protein domains. *J Biol Chem* **274:** 14942–14947

Song BD, Leonard M, Schmid SL (2004a) Dynamin GTPase domain mutants that differentially affect GTP binding, GTP hydrolysis, and clathrin-mediated endocytosis. *J Biol Chem* **279:** 40431–40436

Song BD, Schmid SL (2003) A molecular motor or a regulator? Dynamin's in a class of its own. *Biochemistry* **42:** 1369–1376

Song BD, Yarar D, Schmid SL (2004b) An assembly-incompetent mutant establishes a requirement for dynamin self-assembly in clathrin-mediated endocytosis *in vivo*. *Mol Biol Cell* **15:** 2243–2252

Stowell MH, Marks B, Wigge P, McMahon HT (1999) Nucleotide-dependent conformational changes in dynamin: evidence for a mechanochemical molecular spring. *Nat Cell Biol* **1:** 27–32

Sweitzer SM, Hinshaw JE (1998) Dynamin undergoes a GTP-dependent conformational change causing vesiculation. *Cell* **93:** 1021–1029

Tuma PL, Collins CA (1995) Dynamin forms polymeric complexes in the presence of lipid vesicles. Characterization of chemically cross-linked dynamin molecules. *J Biol Chem* **270:** 26707–26714

Warnock DE, Hinshaw JE, Schmid SL (1996) Dynamin self-assembly stimulates its GTPase activity. *J Biol Chem* **271:** 22310–22314

Warnock DE, Schmid SL (1996) Dynamin GTPase, a force-generating molecular switch. *BioEssays* **18:** 885–893

Wen J, Arakawa T, Philo JS (1996) Size-exclusion chromatography with on-line light-scattering, absorbance, and refractive index detectors for studying proteins and their interactions. *Anal Biochem* **240:** 155–166

Ye H (2006) Simultaneous determination of protein aggregation, degradation, and absolute molecular weight by size exclusion chromatography-multiangle laser light scattering. *Anal Biochem* **356:** 76–85

Ye J, Esmon NL, Esmon CT, Johnson AE (1991) The active site of thrombin is altered upon binding to thrombomodulin. Two distinct structural changes are detected by fluorescence, but only one correlates with protein C activation. *J Biol Chem* **266:** 23016–23021

Zhang P, Hinshaw JE (2001) Three-dimensional reconstruction of dynamin in the constricted state. *Nat Cell Biol* **3:** 922–926

